17E. OSCILLATING 65° DELTA WING, EXPERIMENTAL

Thomas Loeser
German – Dutch Wind Tunnel
DNW - NWB
Braunschweig, Germany

INTRODUCTION

This data set contains force and pressure data resulting from static and dynamic measurements on a sharp-edged cropped delta wing with a leading edge sweep of 65° oscillating in different modes. Motivation for the experiment were the provision of experimental data for validation of unsteady computational codes and understanding of the flow past an oscillating delta wing.

The model geometry is identical to a geometry used in the Vortex Flow Experiment for Computer Code Validation (VFE), a multinational cooperation which provided experimental data of delta wing configurations in the mid eighties [3], [4]. The geometry of the wing is also used for steady and unsteady calculations within the Western European Armament Group (WEAG, formerly IEPG) TA - 15.

The experiments have been performed in 1994 (force measurements) and 1995 (pressure measurements). They were performed in the German-Dutch wind tunnel DNW-NWB at low speeds, the model undergoing pitching, yawing or rolling motions about wind-fixed axes. The choice of the mean angles of attack was closely related to the expected flow types:

$\alpha_0 = 0°$: In this case the vortex formation will alternate between the upper and the lower surface of the configuration during the pitching motion.

$\alpha_0 = 9°$: Vortices will be present over the upper surface of the configuration and no vortex breakdown will occur during the whole cycle of the pitching motion.

$\alpha_0 = 15°$ and

$\alpha_0 = 21°$: These conditions are related to mixed cases without vortex breakdown over the configuration at low angles of attack and with vortex breakdown at high angles of attack during the cycle of motion.

$\alpha_0 = 27°$: Vortices with vortex breakdown are expected to occur over the upper surface of the configuration and this type of flow will be present during the whole cycle of the pitching motion.

$\alpha_0 = 42°$: During the cycle of the pitching motion the flow is expected to switch between a vortex-type flow with vortex breakdown and a dead-water-type flow.

$\alpha_0 = 48°$: In this case a deadwater-type flow is expected during the whole cycle of motion.

The mean angles of attack at which no vortex breakdown occurs during the complete cycle of motion are simpler to treat numerically. Therefore the pitching oscillations about $\alpha_0 = 9°$ was the first case to be included in a WEAG TA-15 common exercise. The other case included in that common exercise is the pitching oscillation about $\alpha_0 = 21°$, the reduced frequency being 0.56 for all mean angles of attack. Results from unsteady Euler and Navier-Stokes calculations of pitching oscillation about $\alpha_0 = 9°$ with an amplitude of $\Delta\alpha = 3°$ by W. Fritz are included in the following chapter 17C.

LIST OF SYMBOLS AND DEFINITIONS

$b = 2s$	wing span
c	chord
c_i	root chord
C_L, C_D, C_m	lift, drag and pitching moment coefficients, reference length for C_m: c_i, see figs. 1 and 3 for reference point
C_Y, C_l, C_n	side force, rolling moment and yawing moment coefficients, reference length for C_l and C_n: s, see figs. 1 and 3 for reference point
C_p	static pressure coefficient, $C_p = (p - p_\infty)/q_\infty$
d	fuselage diameter, see fig. 3
DNW - NWB	Deutsch-Niederländischer Windkanal - Niedergeschwindigkeits-Windkanal Braunschweig
f_0	model oscillation frequency
FS	full scale
F_x, F_y, F_z	forces in x, y, z -direction in balance-fixed coordinate system
LE	leading edge
m0	unsteady mean value of force and pressure values, see fig. 7
m1, m2, m3	amplitudes of the first, second and third harmonic of force and pressure values, see fig. 7
M_x, M_y, M_z	moments about balance-fixed x, y, z-axis
q_∞	dynamic pressure
Re	Reynolds number, $Re = V_\infty \cdot c_i / \nu$
TE	trailing edge
V_∞	free stream velocity
t	time
x, y, z	rectangular wing-fixed coordinate system, origin at apex, see fig. 3
α	angle of attack
α_0	mean angle of attack
$\Delta\alpha$	amplitude of pitching oscillation
β	angle of sideslip

β_0	mean angle of sideslip
$\Delta\beta$	amplitude of yawing oscillation
η	dimensionless span-wise coordinate, $\eta = y/s(x)$
$\Delta\Phi$	amplitude of rolling oscillation
φ_i	phase angle of the *i*th harmonic with respect to the model motion
ω^*	reduced frequency, $\omega^* = 2\pi \cdot f_0 \cdot c_i / V_\infty$ (pitching motion), $\omega^* = 2\pi \cdot f_0 \cdot s/V_\infty$ (yawing and rolling motion)

FORMULARY

1 General description of model

1.1 Designation	VFE WB1 - SLE
1.2 Type	full model
1.3 Derivation	NLR 65°-wing, Ref. 1
1.4 Additional remarks	none
1.5 References	1

2 Model geometry

2.1 Planform	cropped delta wing
2.2 Aspect ratio	1.378
2.3 Leading edge sweep	65°
2.4 Trailing edge sweep	0°
2.5 Taper ratio	0.15
2.6 Twist	0°
2.7 Root chord	1200 mm
2.8 Span of model	951 mm
2.9 Area of planform	0.6564 m^2
2.10 Definition of profiles	symmetrical with sharp leading edge (radius approx. 0.25 mm); 5% rel. thickness; arc segment from leading edge (LE) to x/c = 0.4; airfoil NACA 64A005 from x/c = 0.4 to x/c = 0.75; straight line with 3° inclination from x/c = 0.75 to trailing edge (TE). A sketch of the airfoil including the coordinates of the NACA airfoil used is presented in fig. 8.
2.11 Lofting procedure between reference sections	N/A
2.12 Form of wing-body junction	sharp
2.13 Form of wing tip	square cut
2.14 Control surface details	N/A
2.15 Additional remarks	definition of fuselage: below the wing, the cross section being semicircular at its bottom half and having a constant width at its upper half below the wing. The section of the fuselage protruding above the wing has cylindrical shape again. The fuselage consists basically of three parts: a tapered nose section from $x/c_i = 0.0$ to $x/c_i = 0.358$ (see figs. 2, 3 and 4 for details), a cylindrical section with a width (diameter d) of 160 mm from $x/c_i = 0.358$ to $x/c_i = 1.0$ and a conical section aft of the TE with a length of 50 mm and a taper angle of 15°. The fuselage centreline is located 50 mm below the wing plane ($z/c_i = -0.042$). All dimensions given are nomimal dimensions.
2.16 References	1,2

3 Wind tunnel

3.1 Designation	Low Speed Wind Tunnel Braunschweig DNW - NWB
3.2 Type of tunnel	continuous, atmospheric pressure
3.3 Test section dimensions	height: 2.85 m, width: 3.25 m, Length: 6 m (open) 8 m (closed), open or closed. Open section used.

3.4 Type of roof and floor	open section used
3.5 Type of side walls	open section used
3.6 Ventilation geometry	open section used
3.7 Thickness of side wall boundary layer	open section used
3.8 Thickness of boundary layers at roof and floor	open section used
3.9 Method of measuring velocity	derived from contraction reference pressures
3.10 Flow angularity	0.08°
3.11 Uniformity of Mach number over test section	$\Delta V/V_\infty < 0.1$ % in jet core
3.12 Sources and levels of noise in empty tunnel	no specs
3.13 Tunnel resonances	no evidence of resonance in tests
3.14 Additional remarks	accuracy of wind speed < 0.06 %
3.15 References on tunnel	3

4 Model motion

4.1 General description	
4.1.1 Pitching motion	sinusoidal motion about axis parallel to model Y-axis. Axis location: $x/c_i = 0.5625$, axis located 50 mm ($z/c_i = -0.042$) below wing plane, see fig. 3.
4.1.2 Yawing motion	sinusoidal motion about axis parallel to wind tunnel Z-axis. Oscillation axis intersects with point $x/c_i = 0.5625$, $z/c_i = -0.042$ at all angles of attack, see fig 1.
4.1.3 Rolling motion	sinusoidal motion about axis parallel to wind axis. Oscillation axis intersects with point $x/c_i = 0.5625$, $z/c_i = -0.042$ at all angles of attack, see fig 1.
4.2 Natural frequencies and normal modes of model and support system	no interference with applied frequencies. Lowest natural frequencies above 15 Hz
4.3 Range of amplitude	pitch: 3° and 6°; yaw: 2.5° and 5.0°; roll: 4.5°
4.4.Range of frequency	1.5 Hz and 3.0 Hz, yielding reduced frequencies $0.28 \leq \omega^* \leq 1.12$ (pitching motion), $0.11 \leq \omega^* \leq 0.44$ (yawing and rolling motion)
4.5 Method of applying motion	forced by electric motor
4.6 Timewise purity of motion	fourier analysis of position signal indicates a 2nd harmonic of 0.8%, 1.7% and 3.1% amplitude of the first harmonic and a 3rd harmonic of 0.21%, 0.2% and 0.5% of the first harmonic (typical values for pitching, yawing and rolling motion).
4.7 Actual mode of applied motion including any elastic deformation	see 4.6
4.8 Additional remarks	measurements with oscillating model have been performed in symmetrical flow ($\beta_0 = 0°$)

5 Test conditions

5.1 Model planform area/tunnel area	0.072 (based upon nozzle exit area)
5.2 Model span/tunnel width	0.28
5.3 Blockage	0.56% (frontal blockage) 5 % (projected area at $\alpha = 45°$)
5.4 Position of model in tunnel	standard upright position, center of test section, belly sting axis 2400 mm behind nozzle exit plane
5.5 Range of freestream velocity	20 m/s, 40 m/s 50 m/s at static tests only)
5.6 Range of tunnel total pressure	atmospheric
5.7 Range of tunnel total temperature	293 K ± 5 K
5.8 Range of model incidence	
5.8.1 Range of steady model incidence	$-7.5° < \alpha < 59.2°$

5.8.2 Range of mean model incidence	$\alpha_0 = 0°, 9°, 15°, 21°, 27°, 42°$ (pitching) $\alpha_0 = 9°, 15°, 27°, 42°$ (yawing) $\alpha_0 = 0°, 9°, 27°$ (rolling)
5.9 Definition of model incidence	model incidence defined relative to the wing plane
5.10 Position of transition, if free	not measured
5.11 Position and type of trip, if transition fixed	no trip used
5.12 Flow instabilities during tests	none encountered
5.13 Changes to mean shape of model due to steady aerodynamic load	not measured, negligible
5.14 Additional remarks	none
5.15 References describing tests	2, 4

6 Measurements and observations

6.1 Steady pressures for the mean conditions	yes
6.2 Steady pressures for small changes from the mean conditions	no
6.3 Quasi-steady pressures	yes
6.4 Unsteady pressures	yes
6.5 Steady forces for the mean conditions	
6.5.1 Steady forces for the mean conditions by integration of pressures	no
6.5.2 Steady forces for the mean conditions by direct measurement	yes
6.6 Steady forces for small changes from the mean conditions by integration	no
6.7 Quasi-steady forces by integration	no
6.8 Unsteady forces	no
6.8.1 Unsteady forces by integration	no
6.8.2 Unsteady forces by direct measurement	yes
6.9 Measurement of actual motion at points on model	no
6.10 Observation or measurement of boundary-layer properties	no
6.11 Visualisation of surface flow	yes
6.12 Visualisation of shock wave movements	N/A
6.13 Additional remarks	steady forces and pressures have been measured with increasing angle of attack, control measurements with increasing and decreasing angle of attack have been performed to ensure the absence of hysteresis effects. Forces and pressures have been measured during different wind tunnel entries.

7 Instrumentation

7.1 Steady pressures	pressures for steady conditions measured with same system used for unsteady measurements with the only difference being that the static measurements have been performed with all 10 psi transducers connected simultanously whereas the dynamic measurements have been performed with 2 transducers connected simultanously.
7.1.1 Position of orifices span-wise and chord-wise	see tables 1 and 2.
7.1.2 Diameter of orifices	0.6 mm
7.1.3 Type of measuring system	see 7.2.3
7.2 Unsteady pressures	
7.2.1 Position of orifices span-wise and chord-wise	see tables 1 and 2.
7.2.2 Diameter of orifices	see 7.1.2

7.2.3 Type of measuring system	230 pressure orifices connected with short pressure tubes of equal length to 10 PSI pressure transducers, which are located in the wing of the model. 9 of these orifices are also connected to Kulite pressure transducers by means of tubes of approximately 10 cm length PSI System 780 B, 16bit ADC. Sampling frequencies: 74.35 Hz (PSI), 1000 Hz (Kulites)
7.2.4 Type of transducers	PSI modules used: ESP-16 SL, ESP-32 SL and ESP-48 SL, range: 0.35 psi and 1.0 psi. Kulites used: XCW-062 and XCW 093, range 0.35 bar (= 5.0 psi)
7.2.5 Principle and accuracy of calibration	PSI: 3 calibration pressures (magnitudes adapted to the expected values of the experiment) applied to each module every 30 minutes. Manufacturers claimed accuracy: 0.1 % full scale (FS) worst case, 0.07 % typical, wind tunnel operators checked accuracy: 0.05 % FS Kulite: static calibration at beginning of tunnel entry, offset measurement every 30 minutes.
7.3 Steady forces	steady and unsteady forces measured with six component strain gauge balance of type "Emmen 196-6"
7.4 Unsteady forces	see 7.3
7.5 Model motion	
7.5.1 Method of measurement	spring-loaded foil strain gauges on steel flexures
7.5.2 Accuracy of measured motions	better than 1%
7.6 Processing of unsteady measurements	
7.6.1 Method of acquiring and processing measurements	pressure measurements: see fig 6 force measurements: see fig 6
7.6.2 Type of analysis	fourier analysis, then analysis of variance
7.6.3 Unsteady pressure quantities obtained and accuracies achieved	amplitudes and phases up to the 3rd harmonic. Confidence intervals for amplitudes and phases of each harmonic specified in data files
7.6.4 Method of integration to obtain forces	N/A
7.7 Additional remarks	process of calculating the phase angles of the harmonics: 1. calculate position signal $\alpha(t)$ from raw data 2. calculate Pressure Coefficients -Cp(t) from raw data: $-Cp = (p_\infty - p)/q_\infty$ 3. Set the number of data values to be used for Fourier analysis to cover an integer number of model oscillations 4. Perform Fourier analysis on position signal and calculate phase of its first harmonic according to $\varphi_{1,Pos} = -\text{atan}(Im_{1,Pos}/Re_{1,Pos})$ 5. Perform Fourier analysis on pressure signals -Cp(t). Calculate phase angles of the i-th harmonic according to $\varphi_{i,-Cp} = -\text{atan}(Im_i/Re_i)$. Account for the phase of the position signal by subtracting it from the phases of the harmonics according to $\varphi_{i,-cp} = \varphi_{i,-cp} - i \cdot \varphi_{1,Pos}$. This is equivalent with letting the fourier analysis start at an instant where the position signal has a phase angle $\varphi_{1,Pos}$ of 0°. The phases are then (if necessary) modified to lie again within the range $-180^\circ <= \varphi_{i,-Cp} <= +180^\circ$ 6. The pressure signal now can be represented by $-Cp(t) = -Cp_0 + \sum_{i=1}^{3} -\hat{C}p_i \cdot \cos(i\omega t + \varphi_i)$, $-\hat{C}p_i$ being the amplitude of the i-th harmonic and $-Cp_0$ the constant offset of the signal as presented in the data files. 7. The procedure above applies also to the force measurements. It is important to note the negative sign in the definition of the

	phase angles and the resulting "+" sign in the equation in step 6. Furthermore it should be noted that the phase angles of the harmonics are counted with respect to their maxima, as can be seen in fig. 5.
7.8 References on techniques	7, 8, 9, 10

8 Data presentation

8.1 Test cases for which data could be made available	
8.1.1 Steady pressures	$-6° <= \alpha <= 48°$ in approximately 1° intervals for $\beta = 0°$; $-5° <= \beta <= +5°$ in approximately 1° intervals for $\alpha = 9°$, 15°, 27° and 42°
8.1.2 Unsteady pressures	see tables 4, 6 and 8
8.1.3 Steady forces	$-7.5° <= \alpha <= 58.5°$ in 1.5° intervals at $Re = 1.55 \cdot 10^6$, $Re = 3.1 \cdot 10^6$ and $Re = 3.9 \cdot 10^6$, for $\beta = 0°$; $\beta = -5°, -3°, -3°, 0°, +1°, +3°$ and +5° for $0° <= \alpha <= 54°$ in approx. 3° or 6° intervals for $Re = 3.1 \cdot 10^6$.
8.1.4 Unsteady forces	see tables 3, 5 and 7
8.2 Test cases for which data are included in this document	
8.2.1 Steady pressures	$\alpha = 0°, 9°, 15°, 21°, 27°$ and 42° for $\beta = 0°$, $Re = 1.55 \cdot 10^6$ and/or $Re = 3.1 \cdot 10^6$; $\beta = -5°, 0°, +5°$ for $\alpha = 9°, 15°, 27°$ and 42° for $Re = 3.1 \cdot 10^6$.
8.2.2 Unsteady pressures	see tables 4, 6 and 8
8.2.3 Steady forces	$-7.5° <= \alpha <= 58.5°$ in 1.5° intervals at $Re = 1.55 \cdot 10^6$, $Re = 3.1 \cdot 10^6$ and $Re = 3.9 \cdot 10^6$, $\beta = 0°$; $\beta = -5°$, 0° and +5° for $0° <= \alpha <= 54°$ in approx. 3° or 6° intervals for $Re = 3.1 \cdot 10^6$
8.2.4 Unsteady forces	see tables 3, 5 and 7
8.3 Other forms in which data could be made available	none
8.4 References giving other presentation of data	2
8.5 Additional remarks	force coefficients given for steady measurements at $\beta = 0°$ and for pitching motion: C_L, C_D and C_m; force coefficients given for steady measurements at $\beta \neq 0°$ and for yawing and rolling motion: C_L, C_D C_Y, C_l, C_m, and C_n

9 Comments on data

9.1 Accuracy	
9.1.1 Mach number	see 3.14
9.1.2 Steady incidence	±0.01°
9.1.3 Reduced frequency	±0.1 %
9.1.4 Steady pressure coefficients	see 7.2.5
9.1.5 Unsteady pressure coefficients	confidence interval is result of Analysis of Variance
9.1.4 Steady force coefficients	accuracy according to balance manufacturer: 0.1 – 0.3 % of balance design point values ($F_x = 350$ N, $F_y = 250$ N, $F_z = 1200$ N, $M_x = 100$ Nm, $M_y = 120$ Nm, $M_z = 130$ Nm)
9.1.5 Unsteady force coefficients	confidence interval is result of Analysis of Variance
9.2 Sensitivity to small changes of parameter	no evidence
9.4 Influence of tunnel total pressure	no evidence
9.5 Effects on data of uncertainty, or variation, in mode of model motion	N/A
9.6 Wall interference corrections	no corrections applied
9.7 Other relevant tests on same model	none
9.8 Relevant tests on other models of nominally the same shapes	static tests have been performed within the Vortex Flow Experiment, see references 1, 5, 6
9.9 Any remarks relevant to comparison between	the presence of the fuselage below the wing is believed to be of

experiment and theory	importance for the upper surface flow at small angles of attack and at angles of attack at which vortex breakdown occurs.
9.10 Additional remarks	none
9.11 References on discussion of data	4

Personal contact for further information

Thomas Loeser
DNW - NWB
Lilienthalplatz 7
38108 Braunschweig, Germany
phone: +49 - 531 – 295 - 2454
thomas.loeser@dlr.de

List of references

1 R.H.C.M. Hirdes: US/European Vortex Flow Experiment - Test Report of Wind-Tunnel Measurements on the 65° Wing in the NLR High Speed Wind Tunnel HST; NLR TR 85046 L
2 T. Loeser: Dynamic Force and Pressure Measurements on an Oscillating Delta Wing at Low Speeds; DLR IB 129-96/9
3 G. Kausche, H. Otto, D. Christ, R. Siebert: The Low-Speed Wind Tunnel at DFVLR in Braunschweig (Status 1988); DFVLR-Mitteilung 88-25, 1988
4 D. Hummel, T. Loeser: Low Speed Wind Tunnel Experiments on a Delta Wing Oscillating in Pitch; ICAS-98-3.9.3, Sept. 1998
5 G. Drougge: The international vortex flow experiment for computer code validation; ICAS-Proc. 1988, Vol. 1, pp. XXXV – XLI
6 A. Elsenaar, L. Hjelmberg, K. Bütefisch, W.J. Bannink: The International Vortex Flow Experiment; AGARD-CP-437 (1988), Vol. 1 , pp. 9-1 to 9-23
7 N.L. Johnson, F.C. Leone: Statistics and Experimental Design in Engineering and the Physical Sciences, Vol. II second edition; John Wiley & Sons, New York, 1964
8 R. Mason, R. Gunst, J. Hess: Statistical Design and Analysis of Experiments; John Wiley & Sons, New York, 1989
9 D. Vanmol: Experimental Design and Statistical Analysis applied to Hypersonic Ground Testing; Progress Meeting "Manned Space Transportation Programme", Köln, January 26 & 27 1995
10 H. Coleman, W.G. Steele Jr.: Experimentation and Uncertainty Analysis for Engineers; John Wiley & Sons, New York, 1989

FORMAT OF DATA SET

The static and dynamic pressure and force data are stored in ASCII files. They are located in a directory tree, which is described in a README-file placed in the root directory of this data set. For example, data of dynamic pressure measurements of the pitching motion at 9° mean angle of attack can be found in the subdirectory `pressure/dynamic/pitch/alpha_09`. The naming conventions for the files are also described in the README-file. Additional information with respect to the contents of the files is available at the top of the file, comment lines have a # in the first column. The first lines of a data file containing dynamic pressure data is listed below.

```
################################################################################
#
# Analysis of Variance on constant offset and first 3 Harmonics
# of Magnitudes and Phases of Pressure Coefficients -Cp
# Dimension of Phase Angle : Degrees
# Model                    : VOMO-model WEAG WB1, SLE, Ci = 1200 mm
# Program                  : ./2fd.pl -n -a 27 -f1 theta -f2 omega -d 0 -q 980 -no_wild_plot -print -eps -30o
# Date of Analysis         : Wed Feb 14 00:51:50 MET 1996
#
# alpha                    : 27 degrees
# mode                     : pitch
# Reynolds Number          : 3.10*10^6
# 1. Factor                : theta with levels 3.0 6.0
# 2. Factor                : omega with levels 0.28 0.56
# Prob. for Confid. Inteval: 0.95
# Risk for Significance    : 1 %
# location of pressure taps: x/Ci = 0.3, upper side
#
# Each dim'less spanwise coordinate eta is followed by 7 lines, which
# contain the following data
# m0: Constant Offset of Signal
# m1: Magnitude of 1. Harmonic
# p1: Phase     of 1. Harmonic
# m2: Magnitude of 2. Harmonic
# p2: Phase     of 2. Harmonic
# m3: Magnitude of 3. Harmonic
# p3: Phase     of 3. Harmonic
#
# meaning of the columns:
# 1.column: value for theta 3.0 and omega 0.28
# 2.column: value for theta 3.0 and omega 0.56
# 3.column: value for theta 6.0 and omega 0.28
# 4.column: value for theta 6.0 and omega 0.56
# 5.column: Confidence Interval for above mentioned probability
# 6.column: S, if influence of theta is significant, N if not
```

```
# 7.column: S, if influence of omega is significant, N if not
# 8.column: S, if influence of interaction of theta with omega is significant, N if not
#
#
# eta = +0.000
#
    0.624    0.623    0.626    0.621    +-    0.007  N  N  N
    0.075    0.079    0.162    0.163    +-    0.003  S  N  N
     11.8     14.1      9.3     13.0    +-      2.5  N  S  N
    0.003    0.003    0.003    0.003    +-    0.002  N  N  N
    108.5    101.3     58.7    111.6    +-     51.1  N  S  N
    0.001    0.002    0.005    0.004    +-    0.002  S  N  N
     -9.5    -69.0    -76.0    -93.7    +-     79.9  N  N  N
#
# eta = +0.100
#
    0.627    0.627    0.631    0.627    +-    0.008  N  N  N
    0.077    0.081    0.164    0.166    +-    0.004  S  S  N
     12.5     14.0      9.8     13.4    +-      2.8  N  S  N
    0.003    0.003    0.003    0.003    +-    0.002  N  N  N
    110.0    113.0     44.4     90.5    +-     52.9  S  S  N
    0.001    0.001    0.005    0.003    +-    0.002  S  N  N
    -22.4    -63.0    -70.5    -96.9    +-     87.7  N  N  N
#
```

TABLES

$x/c_i = 0.3$		$x/c_i = 0.6$		$x/c_i = 0.8$	
η	Range / kPa	η	Range / kPa	η	Range / kPa
		-0.980	6.9	-0.980	6.9
-0.960	6.9	-0.960	6.9	-0.960	6.9
-0.940	6.9	-0.940	6.9	-0.940	6.9
-0.920	6.9	-0.920	6.9	-0.920	6.9
-0.900	6.9	-0.900	6.9	-0.900	6.9
-0.875	6.9	**-0.875**	6.9	-0.875	6.9
-0.850	6.9	-0.850	6.9	**-0.850**	6.9
-0.825	6.9	-0.825	6.9	-0.825	6.9
-0.800	6.9	-0.800	6.9	-0.800	6.9
-0.775	6.9	-0.775	6.9	-0.775	6.9
-0.750	6.9	-0.750	6.9	-0.750	6.9
-0.725	6.9	-0.725	6.9	-0.725	6.9
-0.700	6.9	**-0.700**	6.9	**-0.700**	6.9
-0.675	6.9			-0.675	6.9
-0.650	6.9	-0.650	6.9	-0.650	6.9
-0.600	6.9	-0.600	6.9	-0.600	6.9
-0.550	6.9	-0.550	6.9	-0.550	6.9
-0.500	6.9	-0.500	6.9	-0.500	6.9
-0.400	6.9	-0.400	6.9	-0.400	6.9
-0.300	6.9	-0.300	6.9	-0.300	6.9
-0.200	6.9	-0.200	6.9	-0.200	6.9
-0.100	6.9	-0.100	6.9		
0.000	6.9				
+0.100	6.9	+0.100	6.9		
+0.200	6.9	+0.200	6.9	+0.200	6.9
+0.300	6.9	+0.300	6.9	+0.300	6.9
+0.400	6.9	+0.400	6.9	+0.400	6.9
+0.500	6.9	+0.500	6.9	+0.500	6.9
+0.550	6.9	+0.550	6.9	+0.550	6.9
+0.600	6.9	+0.600	6.9	+0.600	6.9
+0.650	6.9	+0.650	6.9	+0.650	6.9
+0.675	6.9			+0.675	6.9
+0.700	6.9	**+0.700**	6.9	**+0.700**	6.9
+0.725	6.9	+0.725	6.9	+0.725	6.9
+0.750	6.9	+0.750	6.9	+0.750	6.9
+0.775	6.9	+0.775	6.9	+0.775	6.9
+0.800	6.9	+0.800	6.9	+0.800	6.9
+0.825	6.9	+0.825	6.9	+0.825	6.9
+0.850	6.9	+0.850	6.9	+0.850	6.9
+0.875	6.9	+0.875	6.9	+0.875	6.9
+0.900	6.9	+0.900	6.9	+0.900	6.9

+0.920	6.9	+0.920	6.9	+0.920	6.9
+0.940	6.9	+0.940	6.9	+0.940	6.9
+0.960	6.9	+0.960	6.9	+0.960	6.9
		+0.980	6.9	+0.980	6.9

Table 1: Location of the pressure taps, upper side, Kulite locations printed bold

$x/c_i = 0.3$		$x/c_i = 0.6$		$x/c_i = 0.8$	
η	Range / kPa	η	Range / kPa	η	Range / kPa
		-0.980	6.9	-0.980	6.9
-0.960	6.9	-0.960	6.9	-0.960	6.9
-0.940	6.9	-0.940	6.9	-0.940	2.4
-0.920	6.9	-0.920	2.4		
-0.900	6.9	-0.900	2.4	-0.900	2.4
		-0.875	2.4	-0.875	2.4
-0.850	2.4	-0.850	2.4	-0.850	2.4
-0.825	2.4	-0.825	2.4	-0.825	2.4
-0.800	2.4	-0.800	2.4	-0.800	2.4
-0.775	2.4	-0.775	2.4		
-0.750	2.4	-0.750	2.4	-0.750	2.4
-0.725	2.4	-0.725	2.4		
-0.700	2.4	-0.700	2.4	-0.700	2.4
-0.675	2.4				
-0.650	2.4	-0.650	2.4	-0.650	2.4
-0.600	2.4	-0.600	2.4	-0.600	2.4
-0.550	2.4	-0.550	2.4	-0.550	2.4
-0.500	2.4	-0.500	2.4	-0.500	2.4
		-0.400	2.4	-0.400	2.4
		-0.300	2.4	-0.300	2.4
				-0.200	2.4
				+0.200	2.4
		+0.300	2.4	+0.300	2.4
		+0.400	2.4	+0.400	2.4
+0.500	2.4	+0.500	2.4	+0.500	2.4
+0.550	2.4	+0.550	2.4	+0.550	2.4
+0.600	2.4	+0.600	2.4	+0.600	2.4
+0.650	2.4	+0.650	2.4	+0.650	2.4
+0.675	2.4				
+0.700	2.4	+0.700	2.4	+0.700	2.4
+0.725	2.4	+0.725	2.4		
+0.750	2.4	+0.750	2.4	+0.750	2.4
+0.775	2.4	+0.775	2.4		
+0.800	2.4	+0.800	2.4	+0.800	2.4
+0.825	2.4	+0.825	2.4	+0.825	2.4
+0.850	2.4	+0.850	2.4	+0.850	2.4
+0.875	6.9	+0.875	2.4	+0.875	2.4
+0.900	6.9	+0.900	2.4	+0.900	2.4
+0.920	6.9	+0.920	2.4		
+0.940	6.9	+0.940	6.9	+0.940	2.4
+0.960	6.9	+0.960	6.9	+0.960	6.9
		+0.980	6.9	+0.980	6.9

Table 2: Location of the pressure taps, lower side

α_0/degrees	Re/10^6	$\Delta\alpha$/degrees
0	**1.6, 3.1**	**6**
9	**1.6, 3.1**	**3,6**
15	**3.1**	**3, 6**
21	**1.6, 3.1**	**6**
27	**1.6, 3.1**	**3, 6**
42	**3.1**	**6**
48	**3.1**	**6**

Table 3: Force Measurements, Pitching Motion

α_0/degrees	Re/10^6	$\Delta\alpha$/degrees
0	**1.6,** 3.1	**6**
9	**1.6, 3.1**	**3, 6**
15	**1.6, 3.1**	**3, 6**
21	**1.6, 3.1**	**3, 6**
27	**1.6, 3.1**	**3, 6**
42	1.6, **3.1**	**6**

Table 4: Pressure Measurements, Pitching Motion

α/degrees	Re/10^6	$\Delta\beta$/degrees
9	1.6, **3.1**	**2.5, 5**
15	**3.1**	**2.5, 5**
27	1.6, **3.1**	**2.5, 5**
42	**3.1**	**5**
48	**3.1**	**5**

Table 5: Force Measurements, Yawing Motion

α/degrees	Re/10^6	$\Delta\beta$/degrees
9	**1.6, 3.1**	**2.5, 5**
15	**1.6, 3.1**	**5**
27	**1.6, 3.1**	**2.5, 5**
42	**1.6, 3.1**	**5**

Table 6: Pressure Measurements, Yawing Motion

α/degrees	Re/10^6	$\Delta\Phi$/degrees
0	1.6, **3.1**	**4.5**
9	1.6, **3.1**	**4.5**
27	1.6, **3.1**	**4.5**

Table 7: Force Measurements, Rolling Motion

α/degrees	Re/10^6	$\Delta\Phi$/degrees
0	1.6, 3.1	4.5
9	**1.6, 3.1**	**4.5**
27	1.6, 3.1	4.5

Table 8: Pressure Measurements, Rolling Motion

All measurements listed in the tables 3 to 8 have been carried out at model oscillation frequencies of f_0 = 1.5 Hz and f_0 = 3.0 Hz. Measurements, which are included in this document, are printed in bold letters.

FIGURES

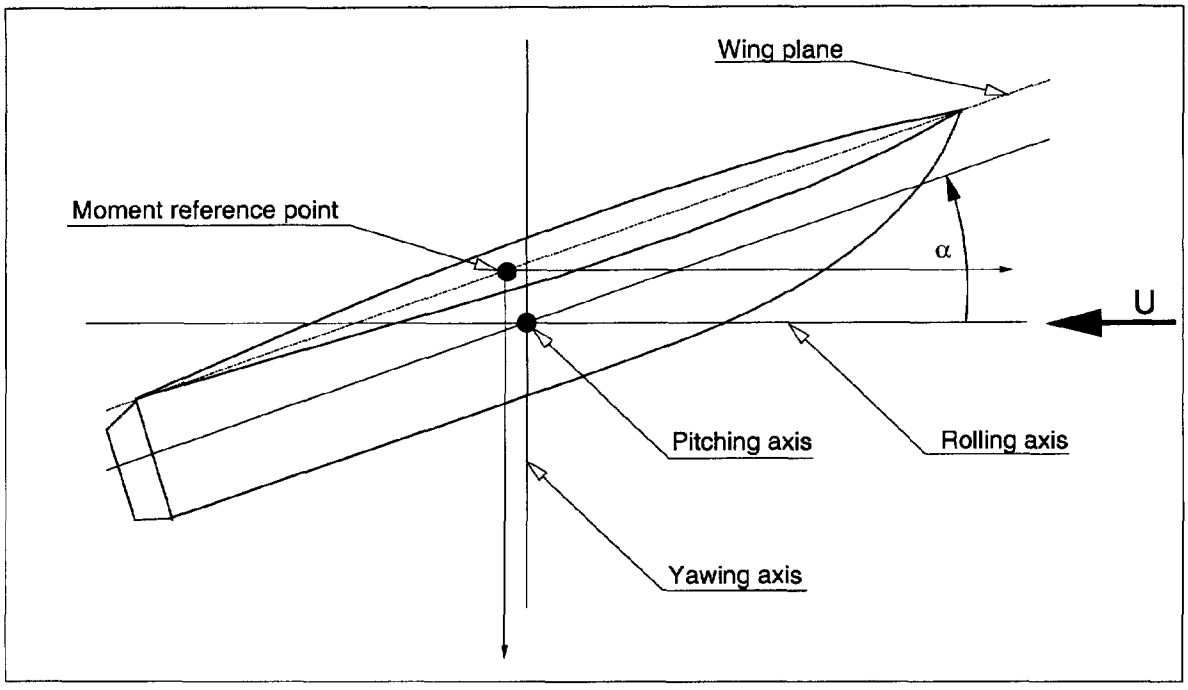

Figure 1: Location of the oscillation axes and the moment reference point

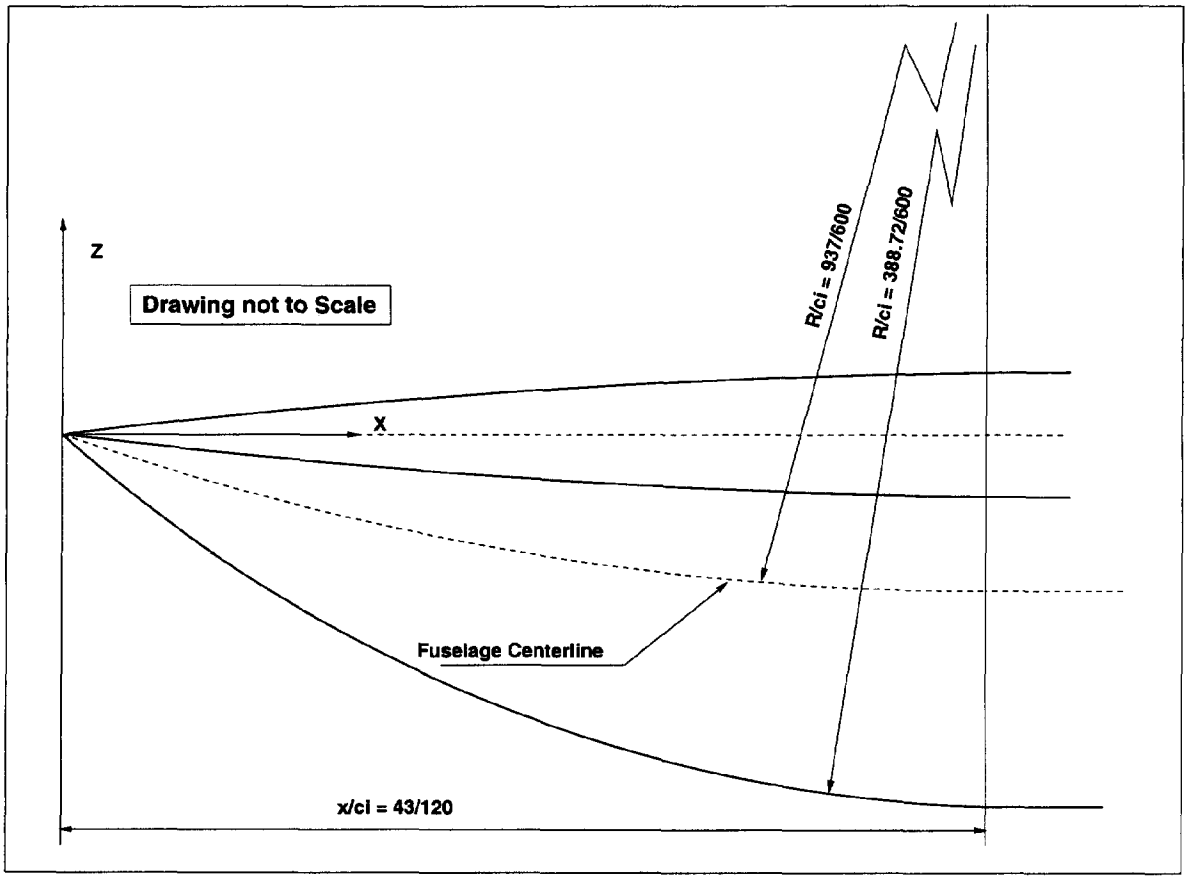

Figure 2: Geometry of the fuselage nose

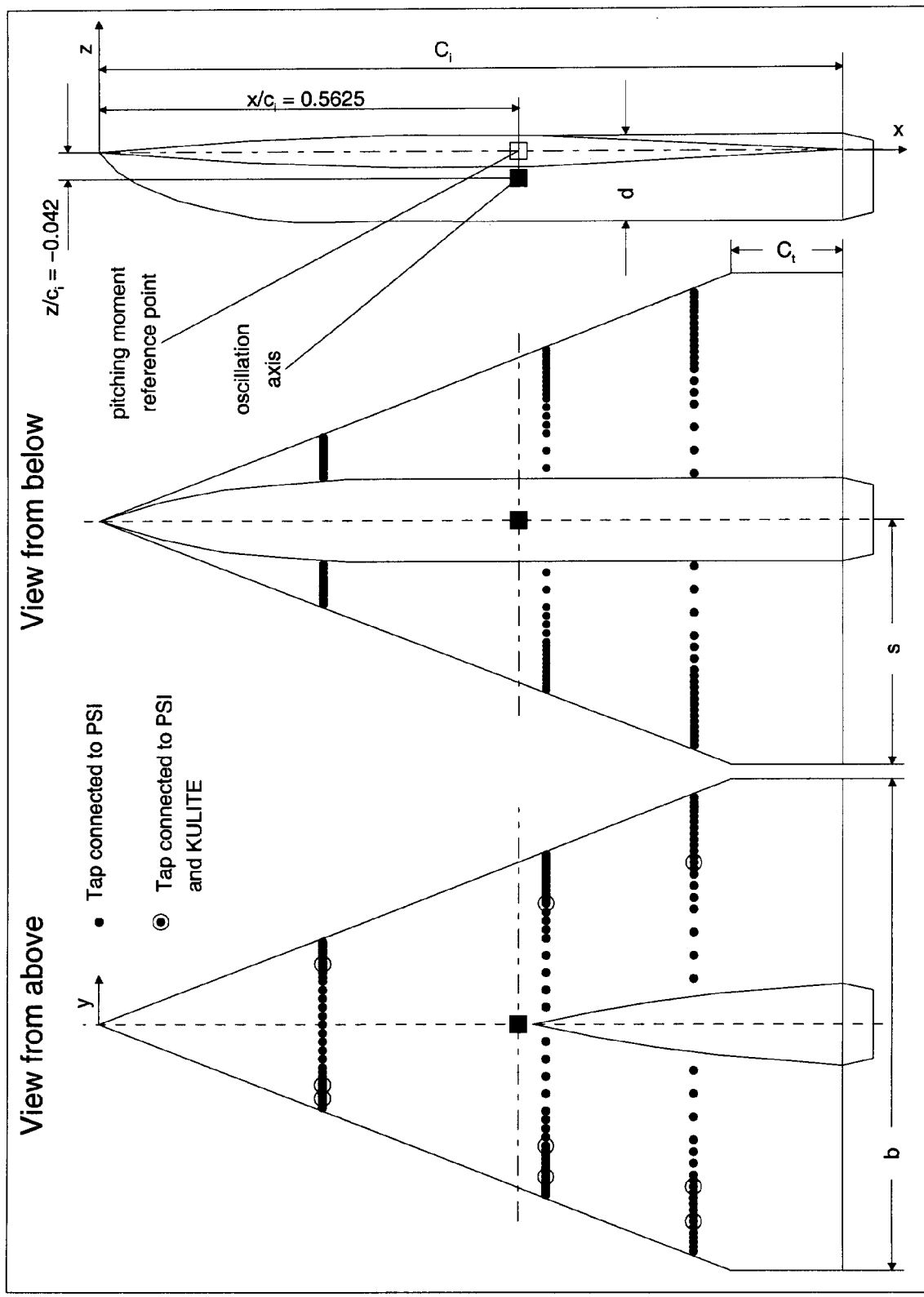

Figure 3: Sketch of the wind tunnel model

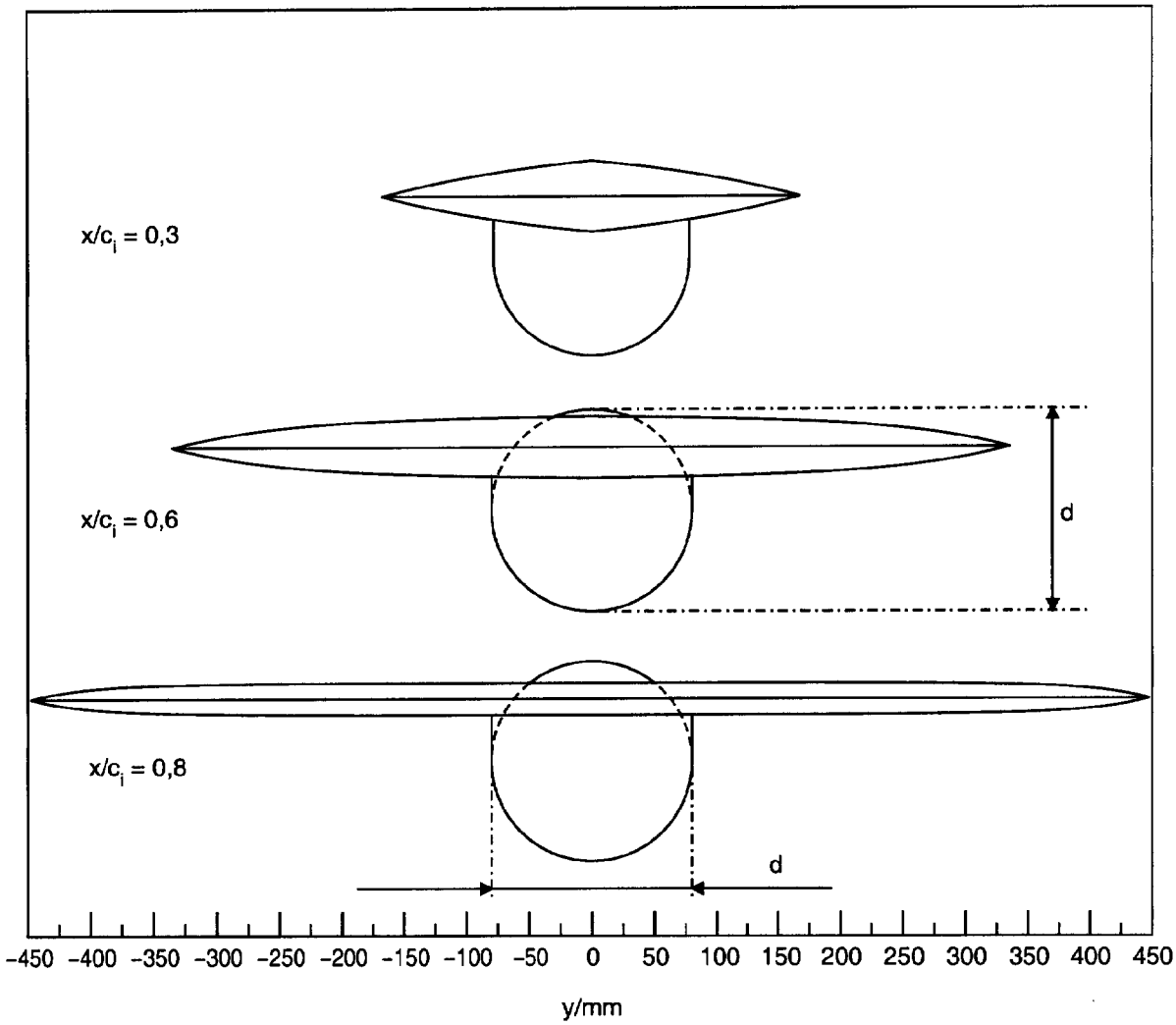

Figure 4: Cross sections of the wind tunnel model at the positions of the pressure taps

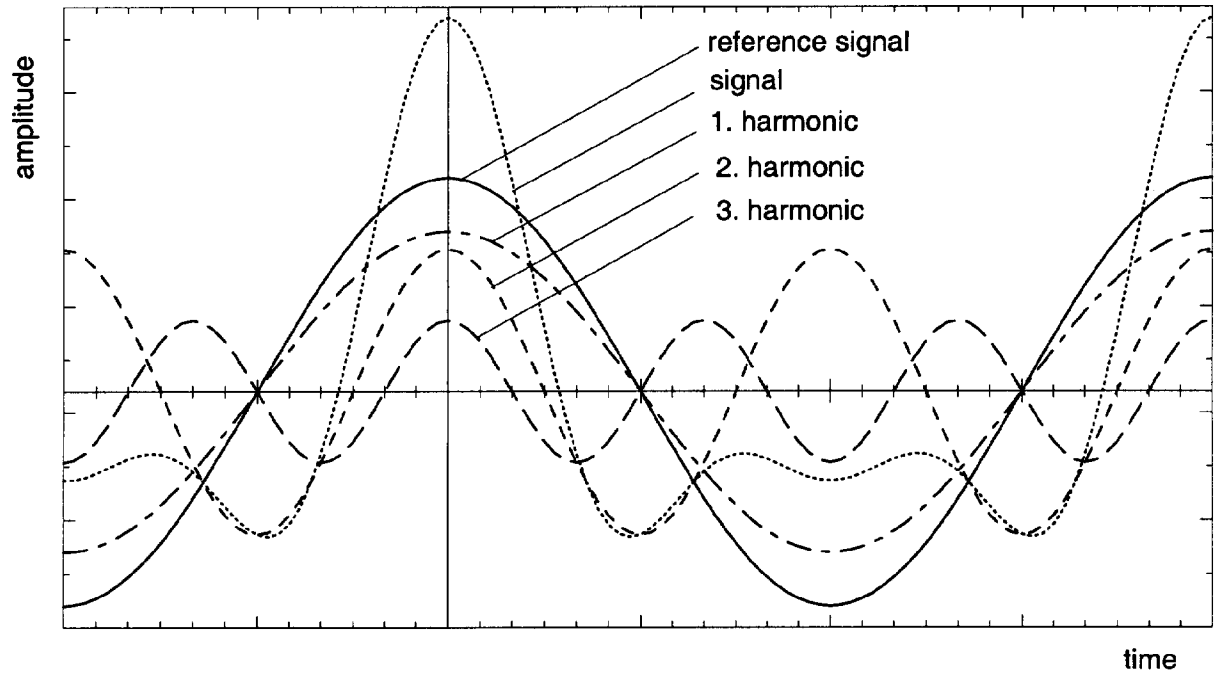

Figure 5: Schematic view of arbitrary signal with harmonics having phase angles $\varphi_i = 0$

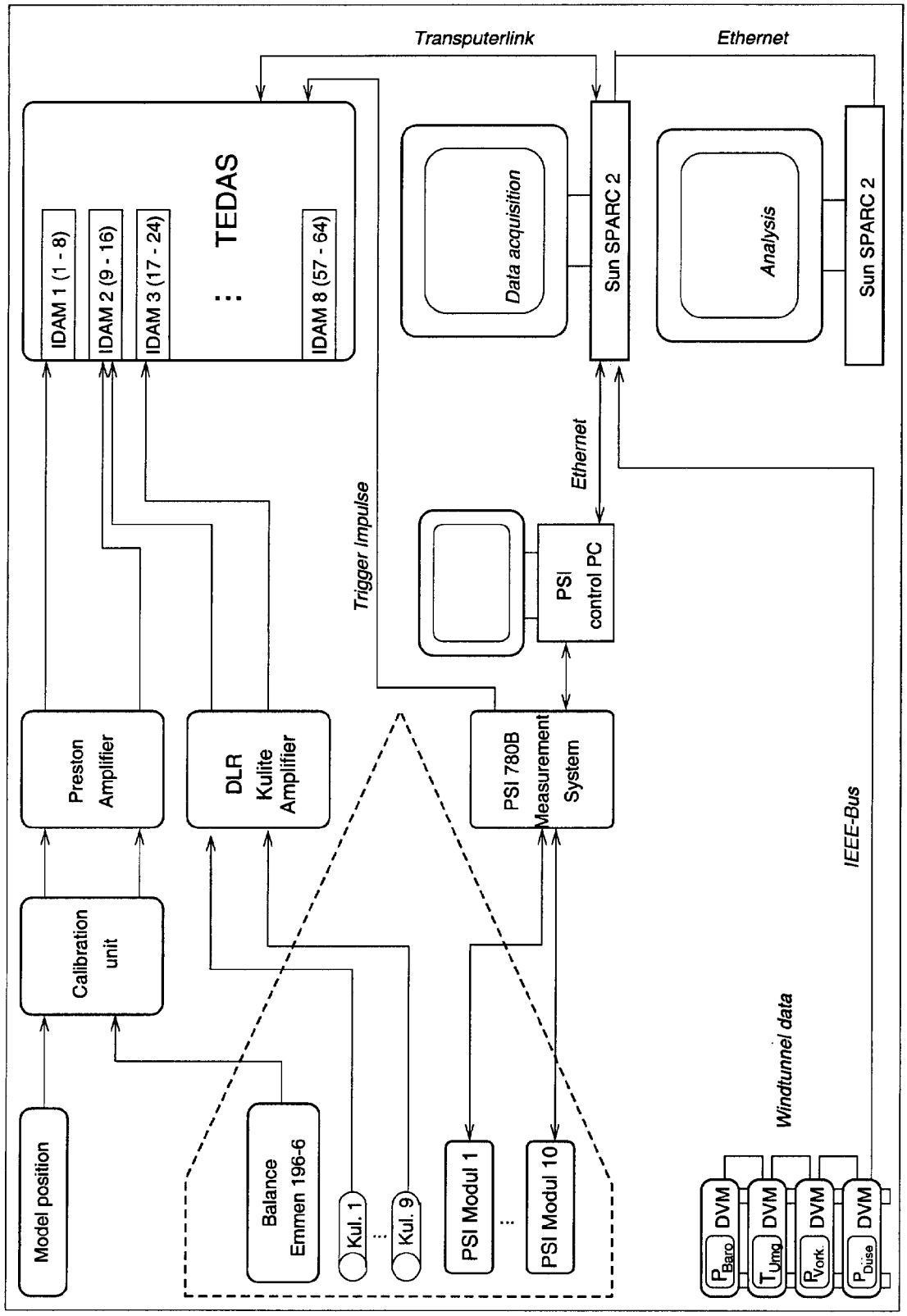

Figure 6: Schematic view of data acquisition

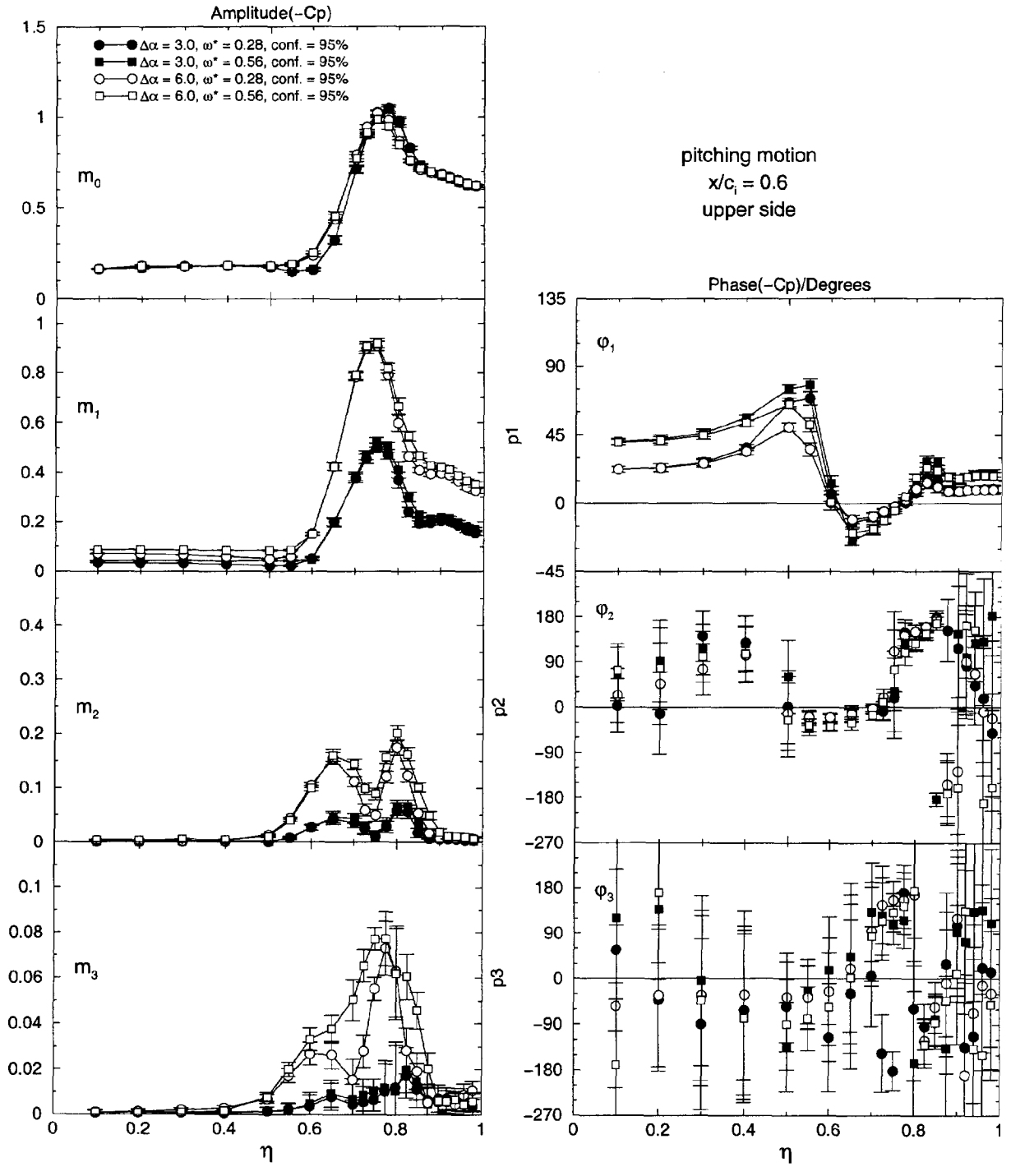

Figure 7: Typical result of an analysis of variance for the unsteady pressure distribution Cp(η) in the section $x/c_i = 0.6$. Pitching motion with $\alpha_0 = 9°$ and factors $\Delta\alpha$ and ω^* at Re = $3.1*10^6$, error bars indicate confidence intervals of 95%. Top to bottom: unsteady mean value, amplitude m1 and phase φ_1 of the first harmonic, amplitude m2 and phase φ_2 of the second harmonic, amplitude m3 and phase φ_3 of the third harmonic.

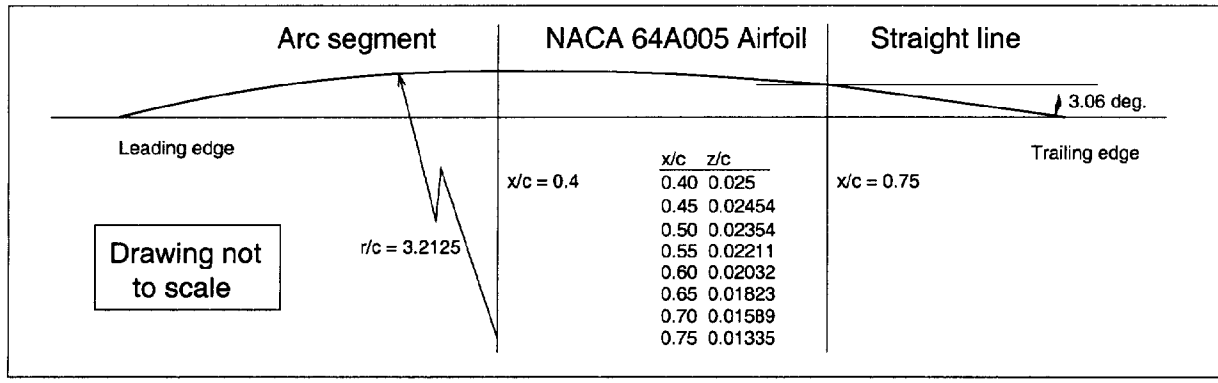

Figure 8: Definition of the airfoil